



## Experimental Investigation of Supercritical Flows at Channel Bends

Prof. Ahmad Wagdy, Dr. Ahmed Helmi, Dr. Ahmed Hussein, Eng. Tarek Abuzaid

Cairo University, Engineering, Irrigation and Hydraulics Dept.

### ملخص عربي

القوة الطاردة المركزية الناتجة عن حركة المياه حول الانحناءات في القنوات المفتوحة تقوم بدفع جزيئات الماء بعيدا عن اتجاه سريان المياه الدائري. من أجل الحفاظ على توازن جزيئات الماء في منطقة الانحناء، تقوم جزيئات المياه بتكوين فرق في الارتفاع بين سطح الماء على طول الجدار الخارجي للمنحنى عن سطح الماء على طول الجدار الداخلي. هذا الارتفاع في سطح الماء يسبب قوة ضغط  $\Delta P$  لتحقيق التوازن مع القوة الطاردة المركزية. ويسمى ارتفاع سطح الماء فوق متوسط عمق المياه Superelevation.

وقد أدى التباين في معادلات حساب Superelevation إلى عدم وجود معايير تصميم و / أو منحنيات تصميمية لتحديد ارتفاع المياه الأقصى على الجدار الخارجي للحركة حول المنحنى؛ وظهور مشاكل في اتخاذ قرار سريع فيما يتعلق بارتفاع الجدران الجانبية أثناء تنفيذ الانحناءات الحادة في القنوات المفتوحة. وبناء على ذلك كان من الضروري تحديد معايير تصميم لتقدير ارتفاع الجدران الخارجية في الانحناءات الحادة في القنوات المفتوحة والتي تظهر في حالة  $r/b < 3$  حيث يحدث اضطرابات عالية في تدفق المياه حول الانحناءات في هذه الحالة.

ولهذا فقد تم اتخاذ مبادرة في هذا البحث لتحديد ارتفاع الجدران الخارجية في الانحناءات في القنوات المفتوحة من خلال إنشاء نموذج معلمي يتكون من قناة مستطيلة بطول 12 م تحتوي في منتصفها على منحنى على درجة 90° ودرجة انحناء  $r/b = 1$  و  $r/b = 2$  وذلك لقياس ارتفاع سطح الماء على زوايا مختلفة داخل المنحنى.

وقد نتج من هذه الدراسة تحديد العلاقة بين Froude No. والنسبة بين عمق المياه الأقصى على الجدار الخارجي من المنحنى وعمق المياه الطبيعي في الجزء المستقيم من القناة.

### Abstract

The centrifugal force generated by flow around a curve will push the water particles away from the stream in a radial direction. In order to maintain water particle equilibrium at the bend section, a differential rise in water surface along the outside wall and depress along the inside wall is created. This water surface rise causes a pressure force  $\Delta P$  to balance the flow against the centrifugal force. The rise of water surface over the mean water depth is called Superelevation.

Discrepancies on the equations for calculating superelevation resulted in the lack of design criteria and/or design charts for determination of water super elevation; and problems in taking fast decision regarding the side walls height during the construction of sharp open channel bends. Accordingly, it is essential to establish design charts for sharp bend, with  $r/b < 3$  where high flow disturbance around bends occurs, to determine the bend side walls height.

Based on that, an initiative has been taken in this research to superelevation in bends through creating a rectangular physical model for measuring the water surface profile for 90° bend with  $r/b=1$  and 2.

The results of this study address a relation between Froude Number and ratio between the maximum water depth and approach depth.

## 1. Introduction

Superelevation is the difference in water-surface elevation between the outside bank and inside bank along a cross section. Figure 1 illustrates superelevation along with the pressure distribution in a meander bend cross section, which creates spiral currents and secondary currents.

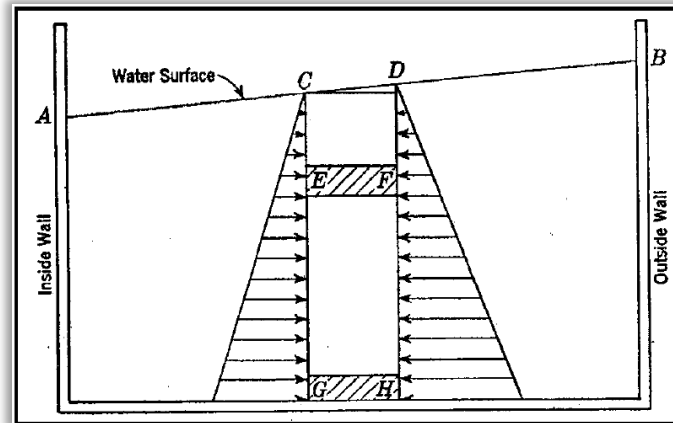


**Figure (1): Pressure Distribution in a Meander Bend (Mockmore, 1944)**

The main common used equation nowadays for computing the superelevation in open channel bends is given by:

$$h_s = \frac{V^2 T}{g r_c} \dots \dots \dots \text{Equation 1}$$

where V is the average velocity in the channel, T is the top width of the channel, and r<sub>c</sub> is the radius of curvature of the centerline of the channel. Equation 1.2 is valid only for subcritical flow conditions, in which case the elevation of the water surface at the outer channel bank is h<sub>s</sub>/2 higher than the centerline water surface elevation, and the elevation of the water surface at the inner channel bank is h<sub>s</sub>/2 lower than the centerline water surface elevation. Equation 1.2 is a theoretical relation derived from the momentum equation (normal to the flow direction) and assumes a uniform velocity and constant curvature across the stream. If the effect of the nonuniform velocity distribution and variation in curvature across the stream are taken into account, the superelevation, h<sub>s</sub>, may be as much as 20% higher than given by Equation 1.2 (Finnemore and Franzini, 2002). In order to minimize flow disturbances around bends, it is also recommended that the radius of curvature be at least three times the channel top width (USACE, 1995).

In this regards:

- A. From theoretical point of view, the discrepancies on the equations for calculating superelevation resulted in the following:
  1. The lack of design criteria and/or design charts for determination of water super elevation at open channel bends,
  2. This lack in design results on the following:
    - a. High costs for over designed side walls at bends,
    - b. Water splashes on roads due to under designed side walls at bends.

- B. From practical point of view; due to steep terrain natures, limited land acquisition, and innovative flood mitigation designs in urban areas, it is essential to focus this study on supercritical flow in Bends with  $rc/b < 3$  where high flow disturbance around bends occurs.

## 2. Study Objective and approach

The main objective of this research is to establish design charts for free board (Side walls height) through determination a relation between Froude No. and the ration between the maximum water depth at the outer bank walls and the water normal depth in the straight parts of an open channel

## 3. Experimental setup and methodology

### 3.1. Physical Model Setup

The experiments reported herein were conducted in a rectangular flume, 0.4 m width, 0.3 m depth [A] and two straight pieces 6.0 m long each [B]. Two bends, 90o angle, 0.4 m wide, and 0.3 m deep, with different curvature radii with the values of 0.4 m and 0.8m[C] was installed in-between the two straight pieces of the flume. This flume will be flexible to create three longitudinal slopes of 0%, 0.4%, and 1%. The flume base and walls were made of steel plate coated by epoxy.

Water was supplied to the flume through (0.10 m) delivery pipe discharging into a steel inlet tank (0.6 m length, 0.3 m width and 0.6 m depth) associated with perforated pipe inlet and two sheets of steel screen 10 cm apart [D]. A multiple layers of 16mm and 10 cm length plastic pipes are located in between the two sheets of steel screen [E] to secure a laminar flow entering to the rectangular flume. At the downstream end of the flume, a tailgate was fixed at the downstream end of the flume [F] to control water level in the flume. This gate is disposing to an exit steel tank (0.9 m length, 0.9 m width and 1.0 m depth) [G]. Both inlet and outlet tanks are rigidly attached to the upstream and downstream ends of the flume, and the whole system is mounted on a steel frame structure of 1.2 m height with eight columns on each piece of the straight flume. These columns were fixed on a screw steel piece which allows vertical displacement of the flume for creating different slopes for the whole system [H].

A large sump tank was constructed at the side of the flume under the laboratory floor. Water was stored in this tank and pumped to the flume via an axial flow vertical pump (30 L/s) maximum capacity, with (6.5 kW) and (2842-rpm) motor [I]. The flow was controlled by a manually operated gate valve, installed on the delivery pipe upstream the flume [J]. The water discharge was measured by a rotated flow meter located on the water delivery pipe upstream of the flume [K]. At the flume top, a movable point gauge was installed [L] to measure the water depth at any point along the flume. Figure 2 and Figure 3 shows a schematic setup illustration and experimental setup photographs, respectively.

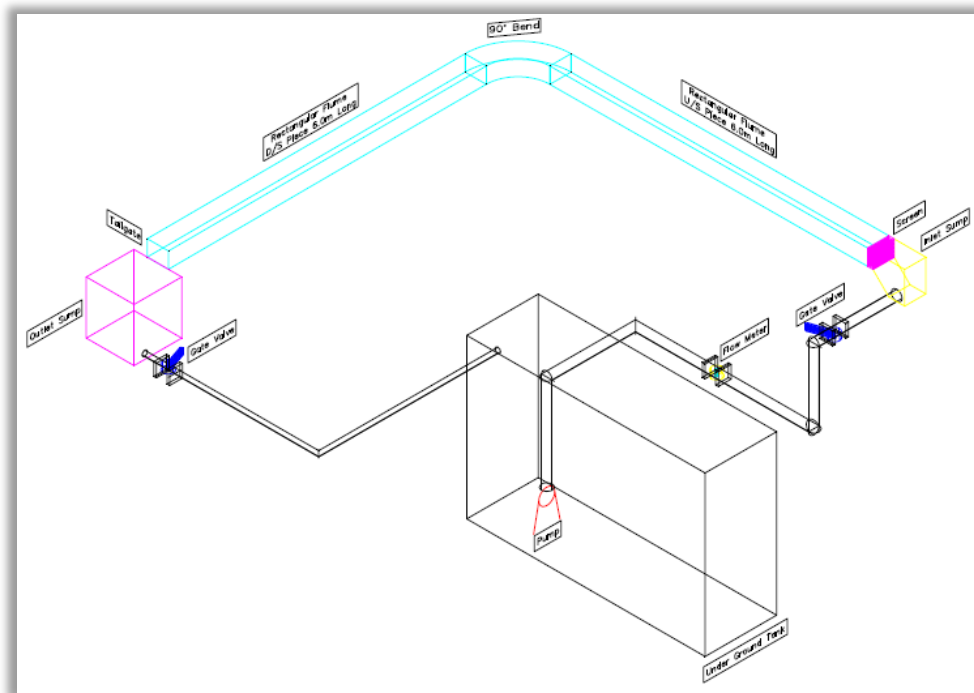
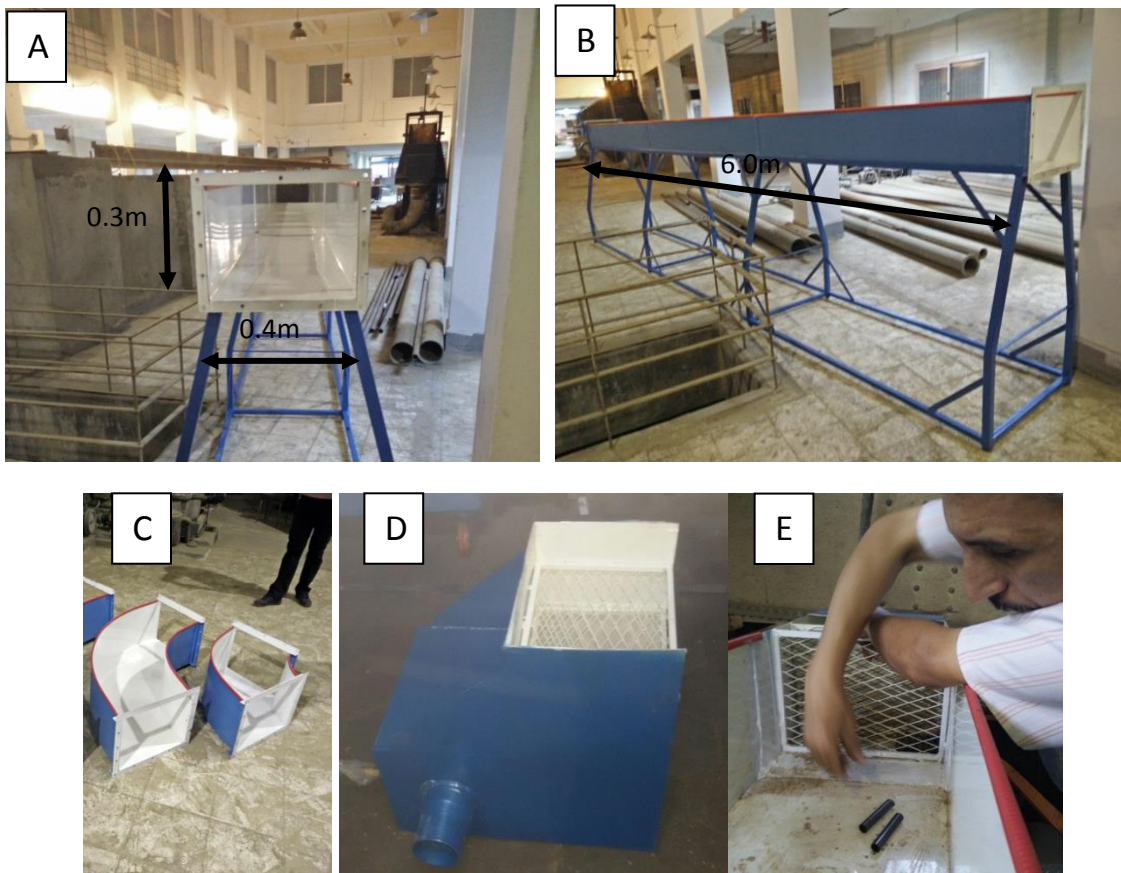
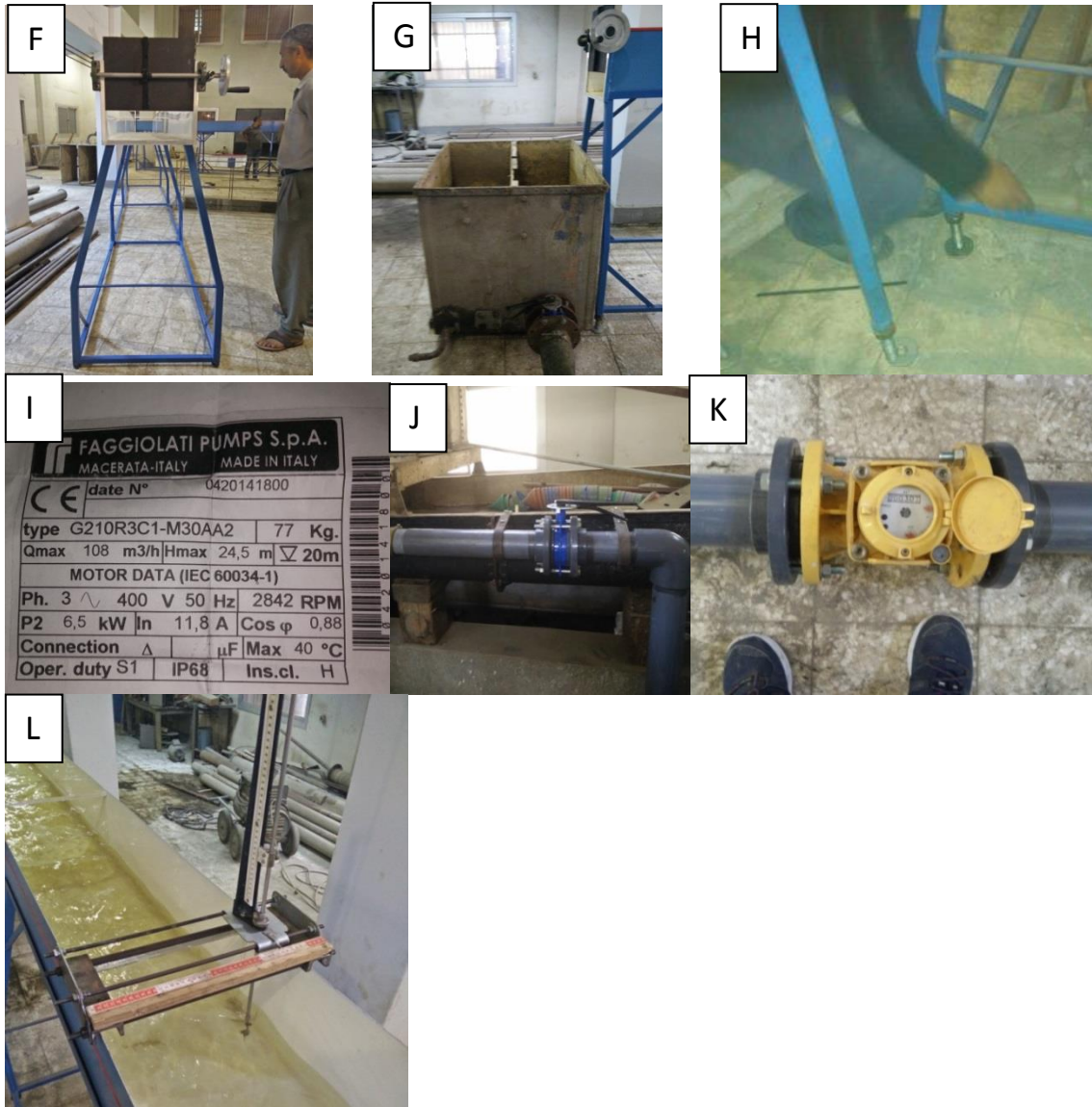


Figure (2): Schematic setup illustration





**Figure (3): Experimental Setup Photographs**

The bends model was fabricated from steel. Three 90° bends was used for the study. The height of the bends is chosen to be 0.3 m in order not to match with the flume height. Each bend is fixed from both sides on the two straight 6.0 pieces and rested on the steel frame with the same height of 1.2m of the whole flume as shown in (Figure 4).



**Figure (4): Photograph for the bend model and its fixation way.**

### 3.2. Test Program

Since the ratio between the bend radius ( $r$ ) and channel width ( $b$ ) is one of the factors affecting the superelevation, two bends are created to be tested in laboratory with ( $r/b$ ) of 1 and 2. Eighteen runs were experimented as shown in the Table (1).

**Table (1) Experimental Runs**

Run No.	$r/b$	S (%)	Q (l/s)	Run No.	$r/b$	S (%)	Q (l/s)
1	1	0	18	10	2	0	18
2	1	0	15	11	2	0	15
3	1	0	12	12	2	0	12
4	1	0.4	18	13	2	0.4	18
5	1	0.4	15	14	2	0.4	15
6	1	0.4	12	15	2	0.4	12
7	1	1	18	16	2	1	18
8	1	1	15	17	2	1	15
9	1	1	12	18	2	1	12

At each run, the longitudinal water surface profiles through the center of flume were recorded via measuring the bed level and water level at 50 points along the flume. Moreover, the transversal water surface profiles were recorder at the 22 cross sections located as shown in the Table (2) and figure (5).

**Table (2) Locations of cross sections**

Section No.	Location	
	W.R.T. Bend Location	Distance from Flume Entrance (m)
1	Upstream the Bend	2.5
2		4.4
3		4.6
4		4.8
5		5.2
6		5.5
7		5.85
8	Within Bend	10°
9		20°
10		30°
11		40°
12		50°
13		60°
14		70°
15		80°
16	Downstream the Bend	7.2
17		7.4
18		7.6
19		7.8
20		8
21		8.4
22		9.7

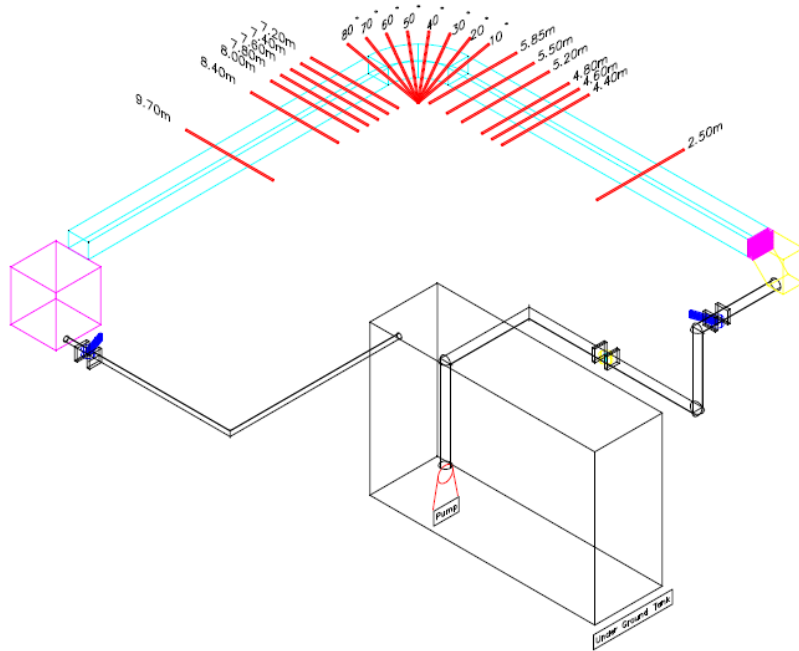


**Figure (5): Locations of cross sections**

## 4. Physical Model Results

The results include; the maximum water depth variation along bend cross section, Maximum water depth variation with flow rate, the location of maximum water depth along the bend region, and the relation between maximum water depth and Froude Number for different r/b ratio.

### 4.1 Maximum water depth variation along bend cross section

The variation of maximum water depth have been measured along the cross sections of the bend for different flow rates for  $r/b = 2$  as illustrated in figures from 2 to 15.

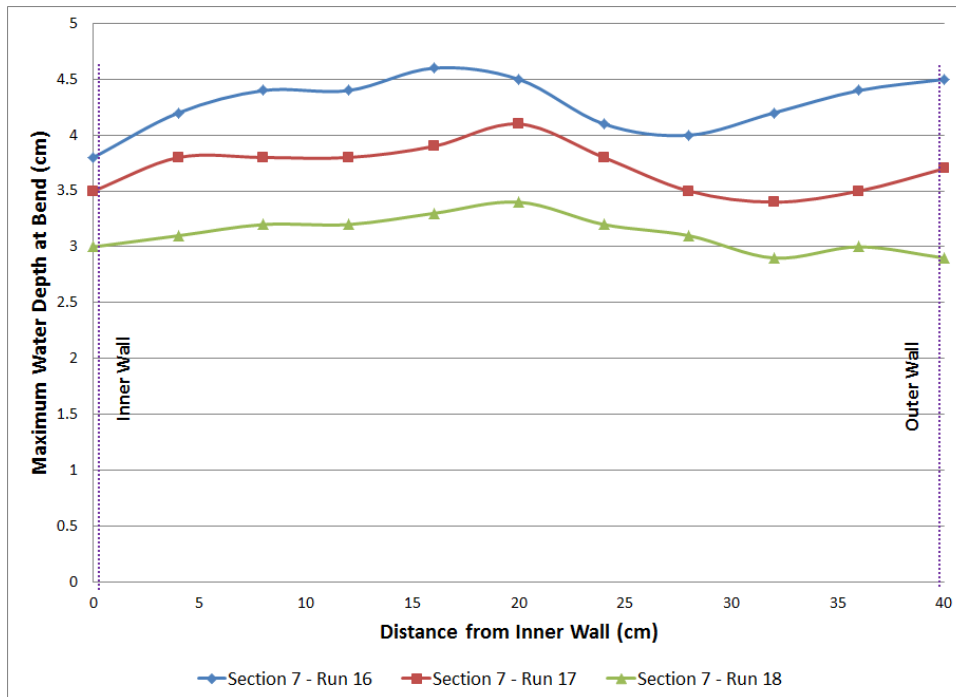
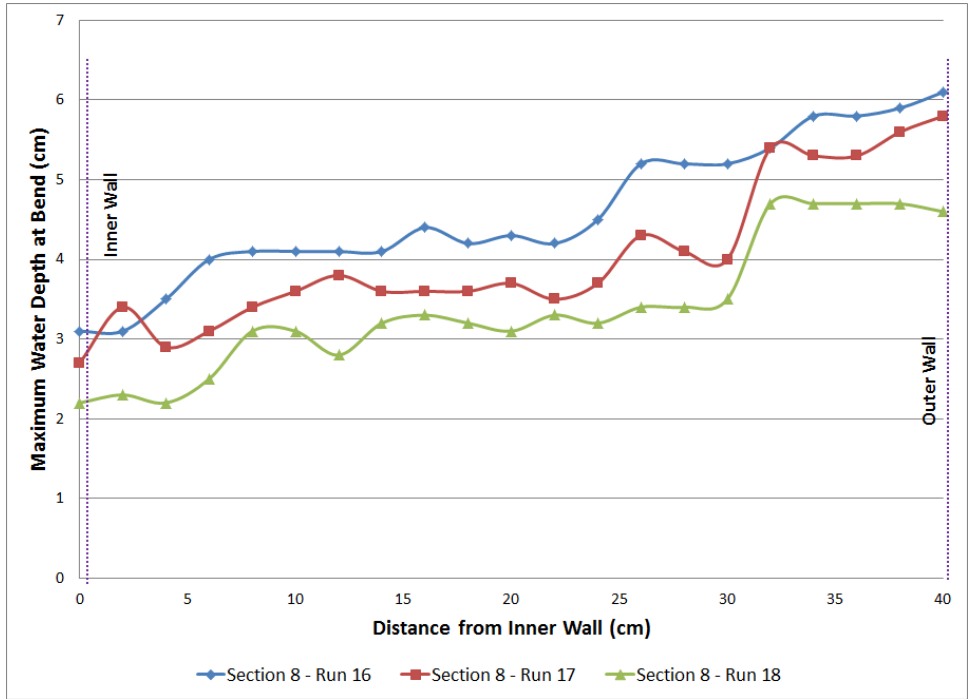
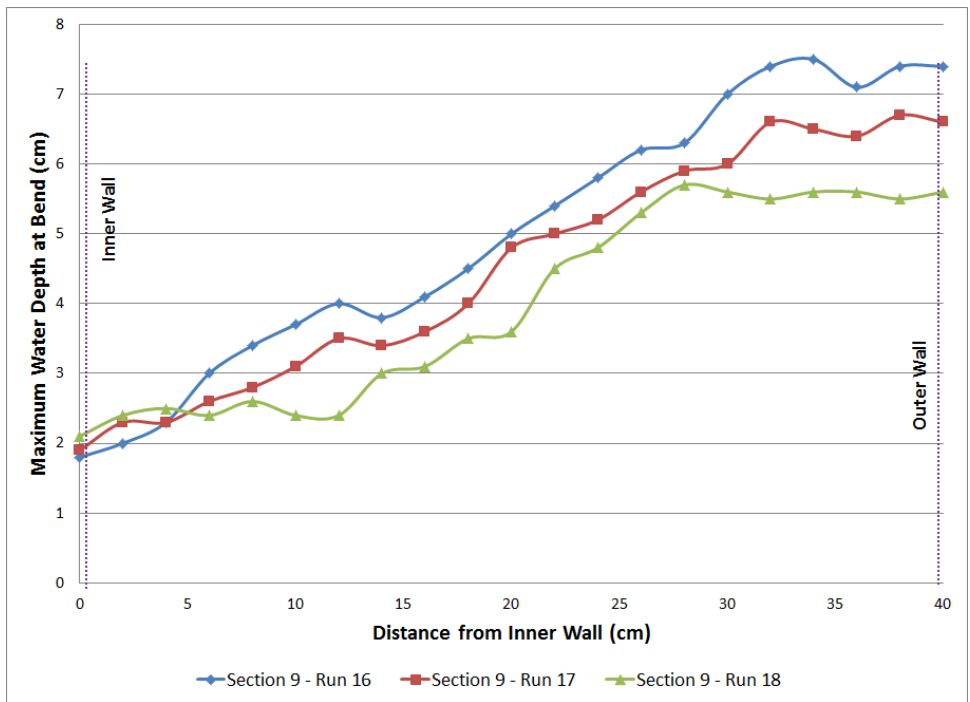


Figure (6): Maximum Water Depth @ section 7 for  $r/b = 2$



**Figure (7): Maximum Water Depth @ section 8 for  $r/b = 2$**



**Figure (8): Maximum Water Depth @ section 9 for  $r/b = 2$**

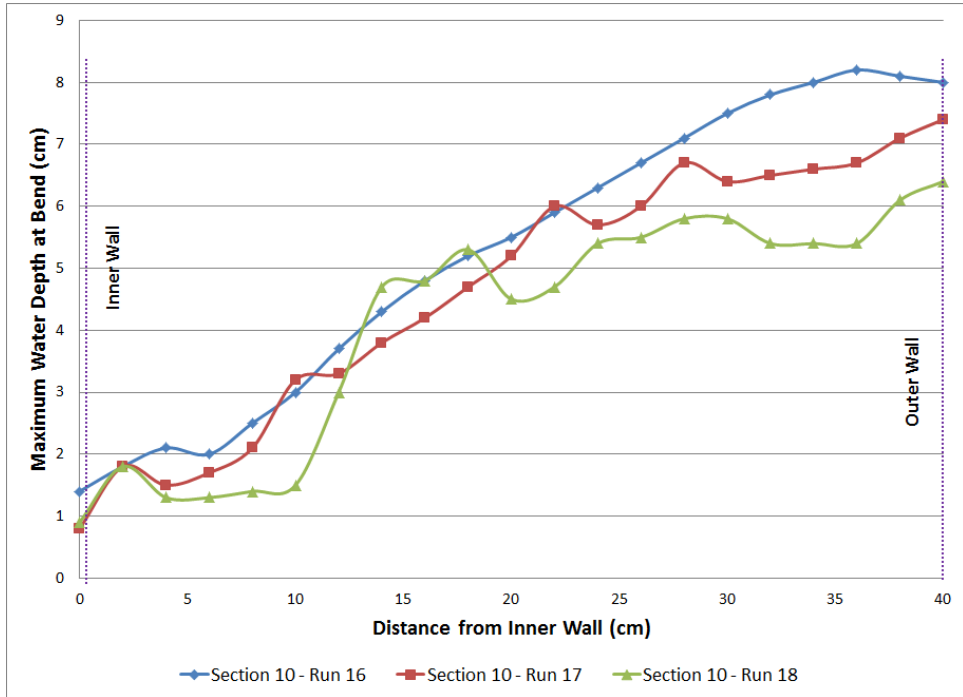


**Figure (9): Maximum Water Depth @ section 10 for  $r/b = 2$**

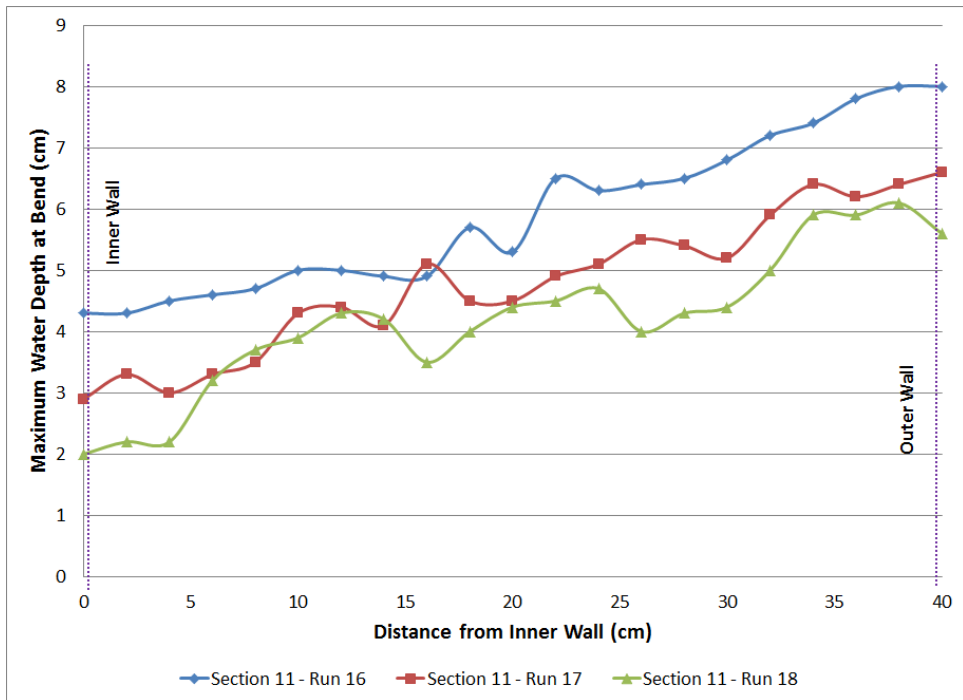


**Figure (10): Maximum Water Depth @ section 11 for  $r/b = 2$**

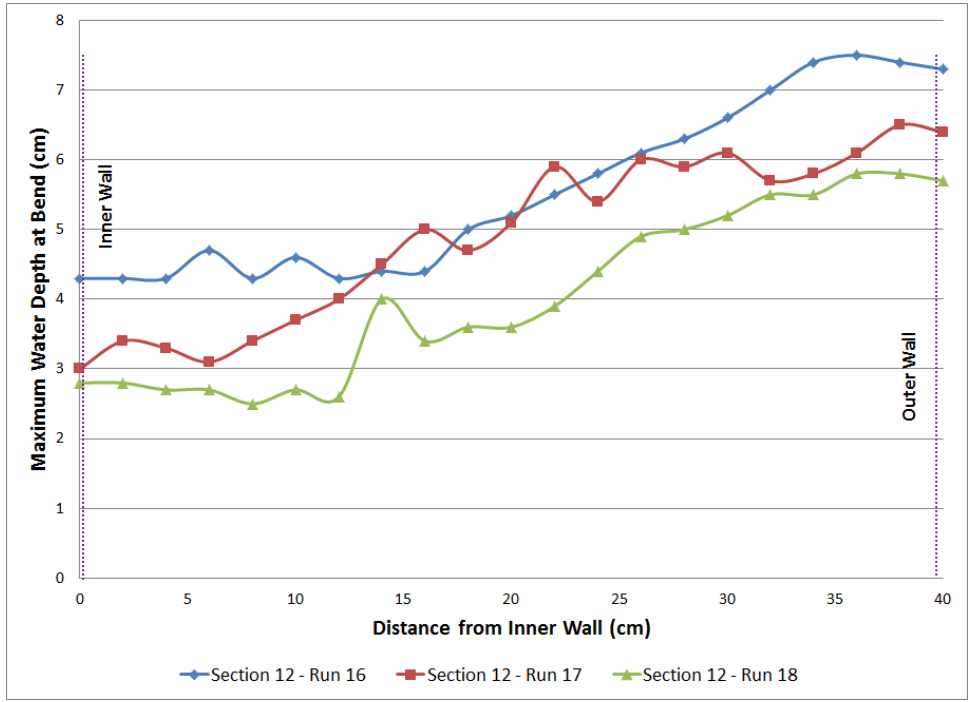


**Figure (11): Maximum Water Depth @ section 12 for  $r/b = 2$**

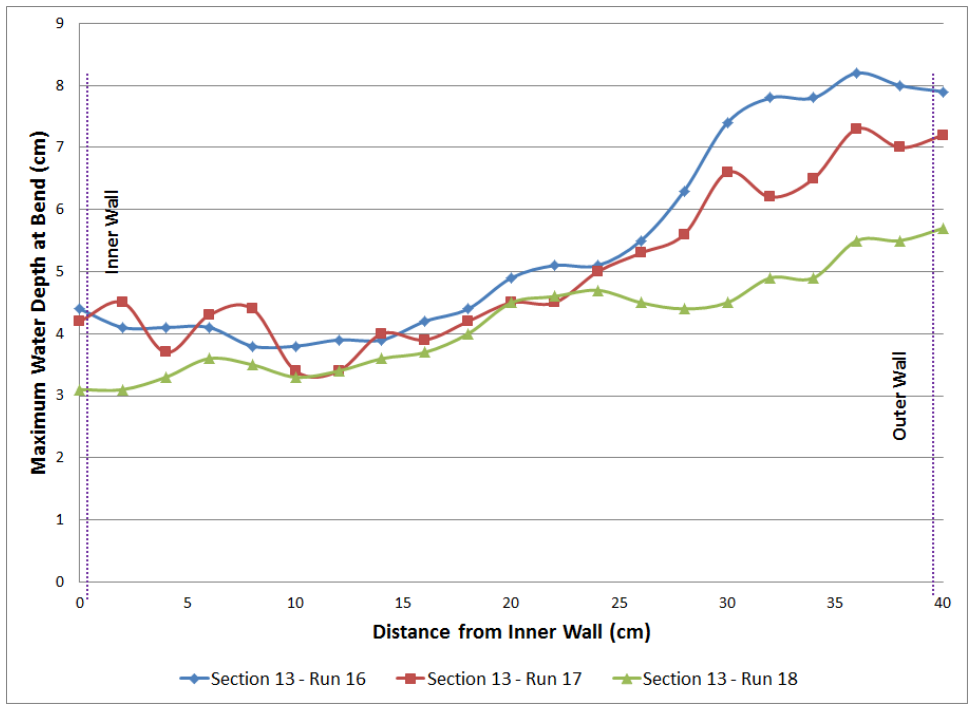


**Figure (12): Maximum Water Depth @ section 13 for  $r/b = 2$**

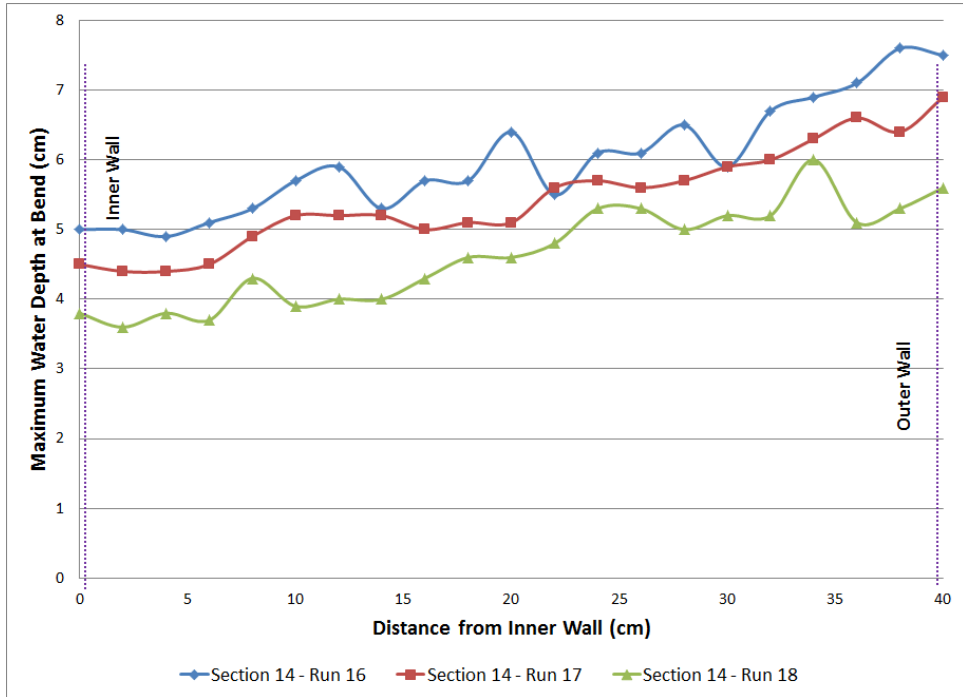


**Figure (13): Maximum Water Depth @ section 14 for  $r/b = 2$**

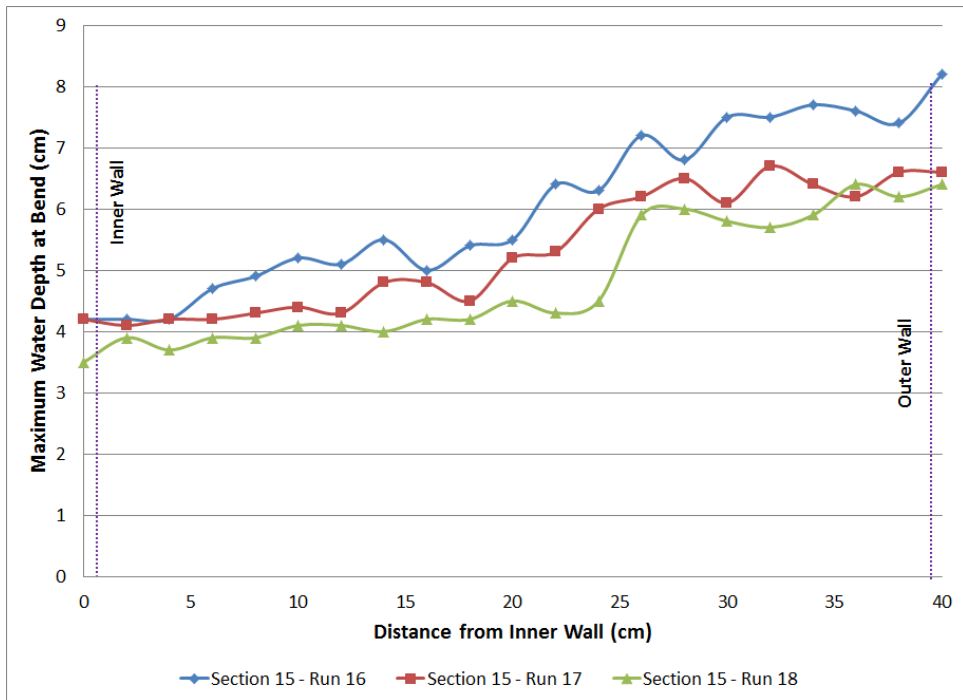


**Figure (14): Maximum Water Depth @ section 15 for  $r/b = 2$**

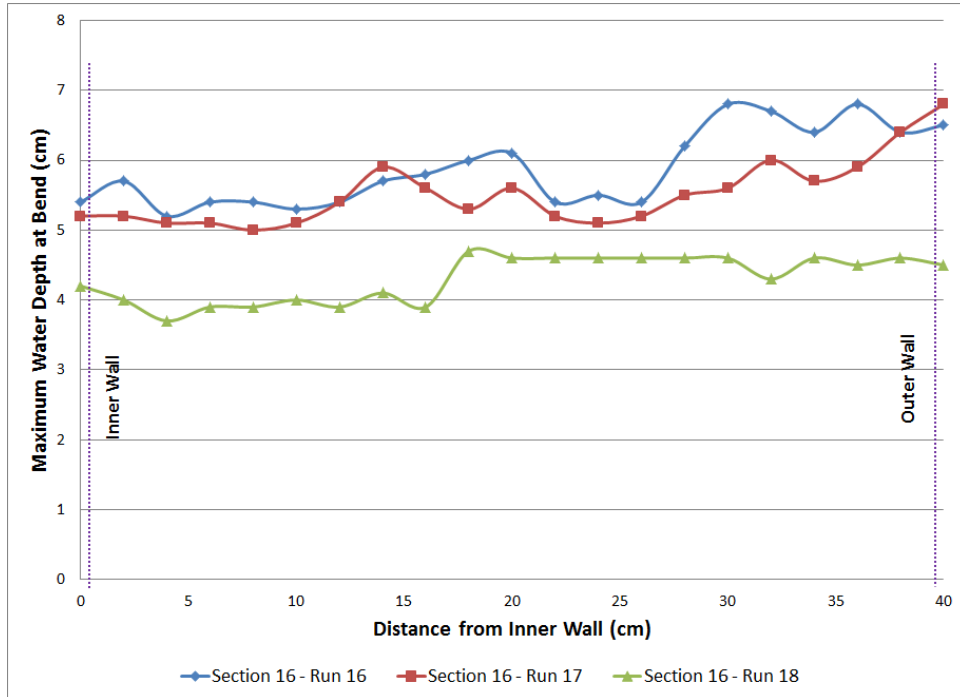


**Figure (15): Maximum Water Depth @ section 16 for r/b = 2**

#### 4.2 Maximum water depth variation with flow rate

The empirical equation relating the maximum water depth along the different bend cross sections and the flow rates for different r/b have been measured as illustrated in figure 16 and figure 17.

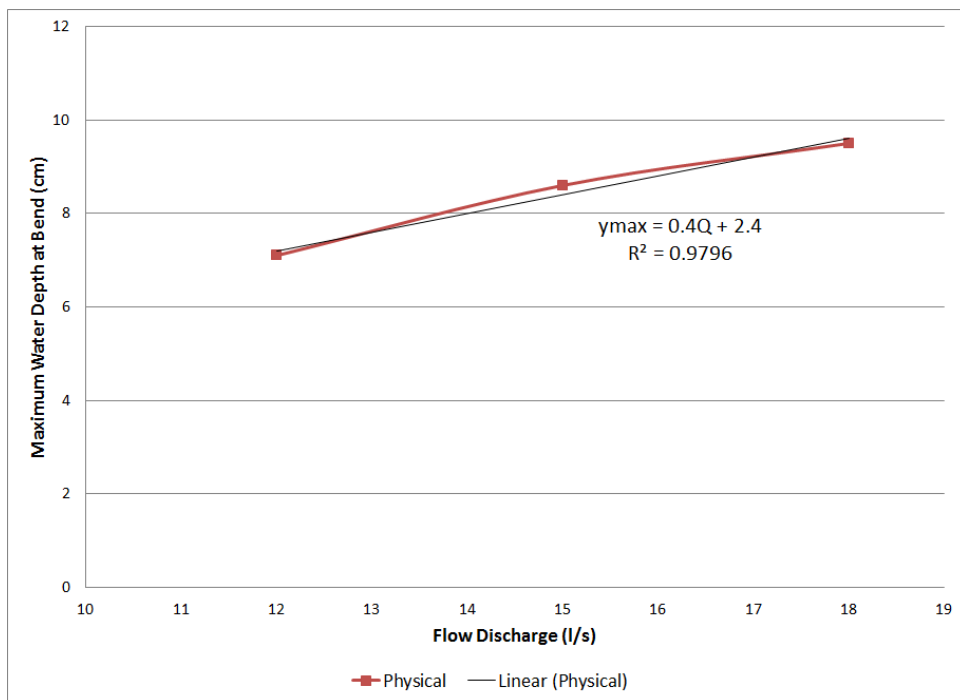


**Figure (16): Flow Discharge VS Max. Water Depth @ Bend for r/b = 1**

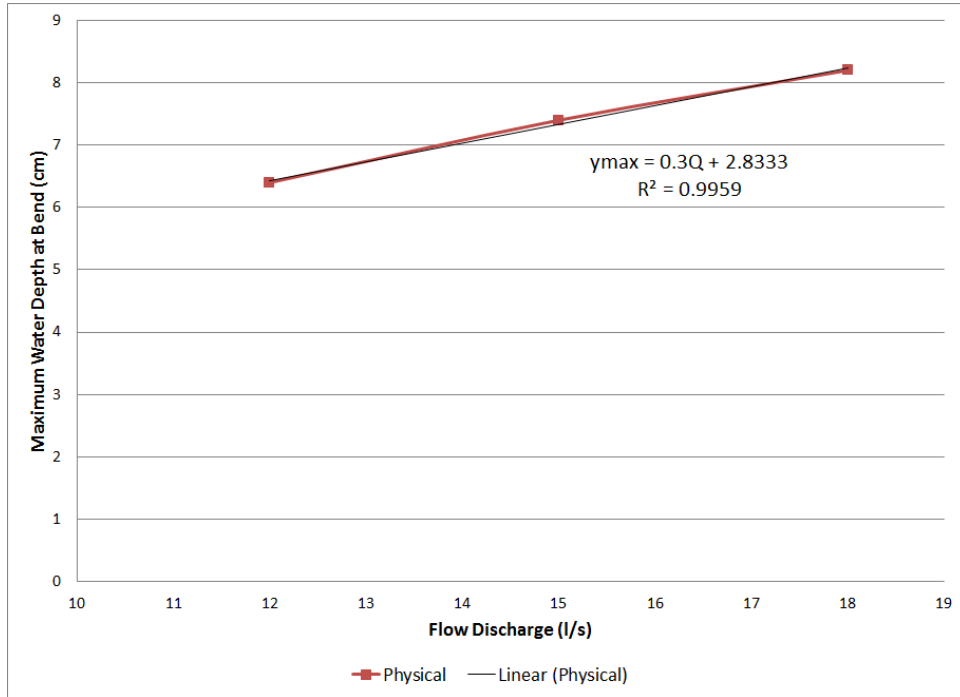


**Figure (17): Flow Discharge VS Max. Water Depth @ Bend for  $r/b = 2$**

### 4.3 Location of maximum water depth along the bend region

The location of maximum water depth have been measured along the bend region for different flow rates and different  $r/b$  as illustrated in figure 18 and figure 19.

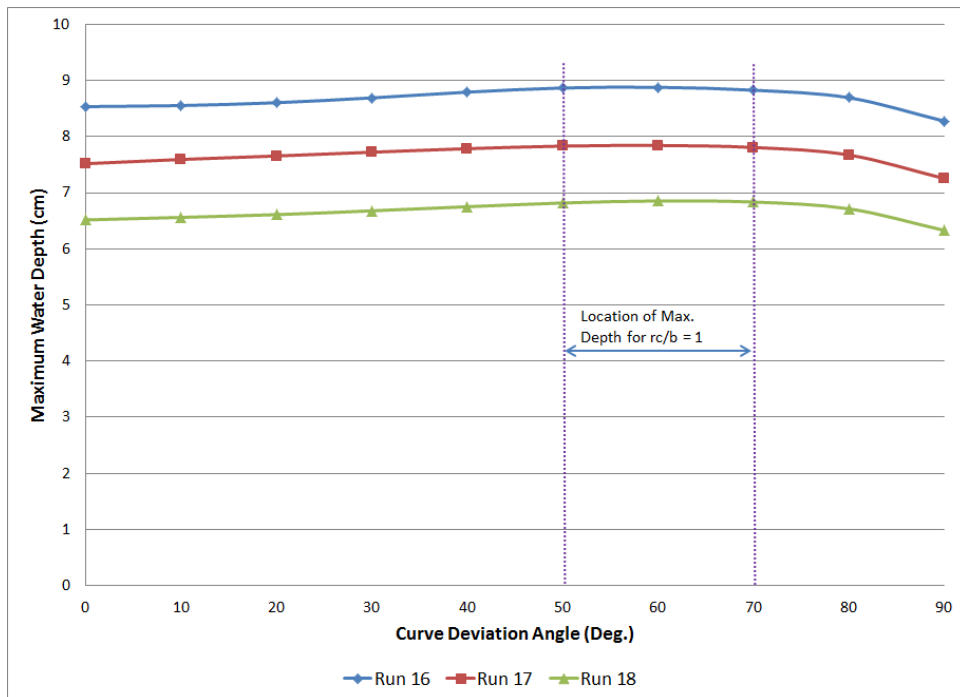


**Figure (18): Location of maximum water depth @ Bend for  $r/b = 1$**

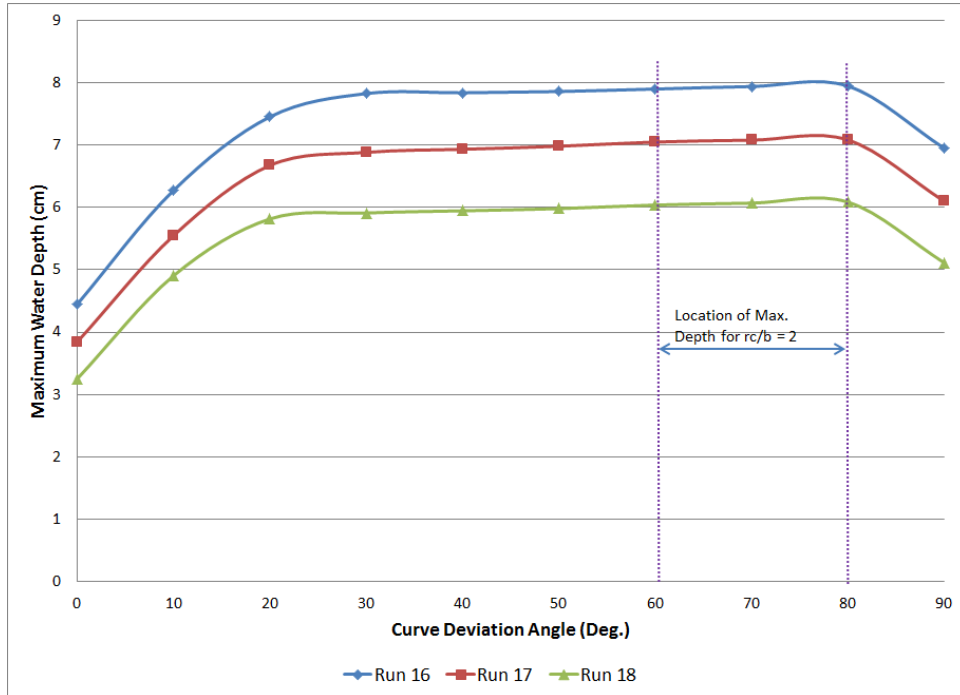


Figure (19): Location of maximum water depth @ Bend for r/b = 1

#### 4.4 Relation between maximum water depth and Froude Number for different r/b ratio

The relation between the maximum water depth at bend and Froude Number has been measured different flow rates and different r/b as illustrated in figure 20.

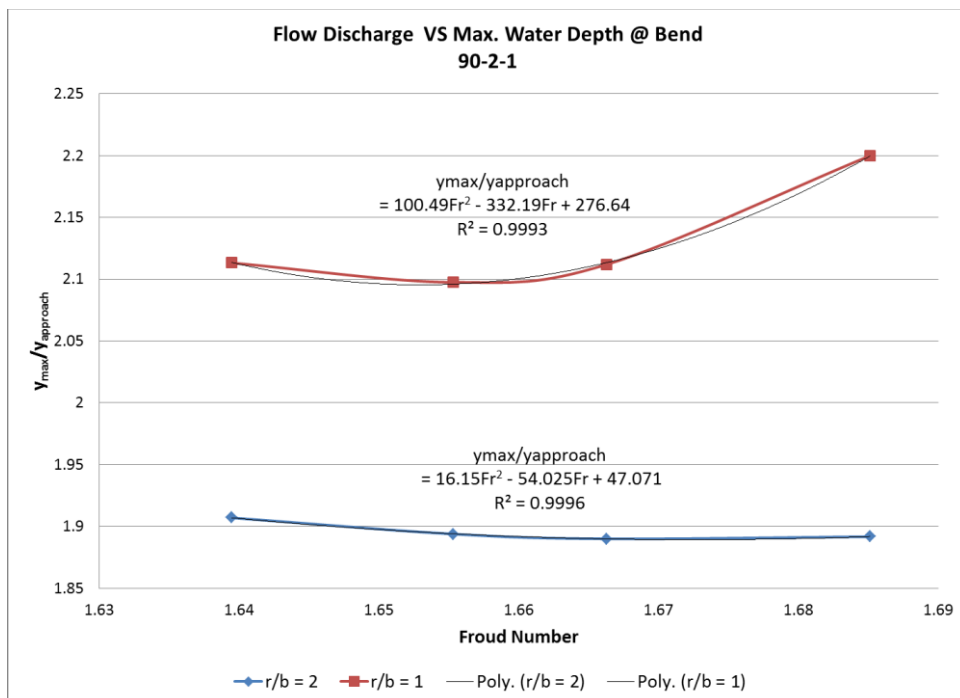


Figure (20): Maximum water depth at bend vs. Froude Number

## 5. Conclusion

The Main conclusions are summarized as follows:

1. The maximum water depth along the bend is nearby the outer wall of the bend, and as the flow rate increase the maximum water depth increase. At the bend exit, the water depth at the outer wall begins to balance to return back to the normal configuration as same as the bend upstream.
2. The maximum water depth in a bend increases linearly with the open channel flow rate, and as  $r/b$  increases, the maximum water depth decreases. The empirical relation between the maximum water depth and the flow rate for different  $r/b$  can be described in empirical equations 2 and 3.

$$y_{max} = 0.4Q + 2.4 \quad \text{for } \frac{r}{b} = 1 \dots \dots \dots \text{Equation 2}$$

$$y_{max} = 0.3Q + 2.8333 \quad \text{for } \frac{r}{b} = 2 \dots \dots \dots \text{Equation 3}$$

3. The maximum water depth along the open channel bend is located between the curve deviation angle of  $50^\circ$  and  $70^\circ$  for  $r/b = 1$ , while it is located between the curve deviation angle of  $60^\circ$  and  $80^\circ$  for  $r/b = 2$ .
4. The relation between the maximum water depth at bend and Froude Number for different flow rates and different  $r/b$  can be described in equations 4 and 5.

$$\frac{y_{max}}{y_{approach}} = 100.49F_r^2 - 332.19F_r + 276.64 \quad \text{for } \frac{r}{b} = 1 \dots \dots \text{Equation 4}$$

$$\frac{y_{max}}{y_{approach}} = 16.15F_r^2 - 54.025F_r + 47.071 \quad \text{for } \frac{r}{b} = 2 \dots \dots \text{Equation 5}$$

## 6. References

1. Lai, Y and Weber, L.J. and Patel, V.C.: Nonhydrostatic Three Dimensional Model for Hydraulic Flow Simulation 1: Formulation and Verification. J. Hyd. Eng., ASCE, 129(3), (2003) 196–200
2. Blanckaert, K., and Graf, W. H. (2001). “Experiments on flow in a strongly curved channel bend.” Proc., 29th Congr. Int. Assoc. Hydr. Res. and Engr., Chinese Hydraulic Engineering Society, Beijing, China (in press).
3. Lien, H.C., Hsieh, T., Y., Yong, J.C. and Yeh, K.C.: Bend-Flow Simulation Using 2D Depth-Averaged Model. J. Hyd. Eng., ASCE, 125(10), (1999) 1097–1108
4. Blanckaert, K., and Graf, W. H. (1999a). “Experiments on flow in open channel bends.” Proc., 28th Congr. Int. Assoc. Hydr. Res., Technical University of Graz, Austria (CD-ROM).
5. Blanckaert, K., and Graf, W. H. (1999b). “Outer-bank cell of secondary circulation and boundary shear stress in open-channel bends.” Proc., Symp. on River, Coastal and Estuarine Morphodynamics, University of Genova, Italy, Vol. 1, 533–543.
6. Y. Shimizu, T. Itakura: Calculation of Bed Variation in Alluvial Channels, J. Hydraul. Eng.115(3), (1989) 367-384
7. Anwar, H. O. (1986). “Turbulent structure in a river bed.” J. Hydr. Engr., ASCE, 112(8), 657–669.
8. de Vriend, H. J., and Struiksma, N. (1984). “Flow and bed deformation in river bends.” River meandering, C. M. Elliot, ed., ASCE, New York, 810–828.

9. Rodi, w., and Leschziner, M. A.: Calculation of Strongly Curved Open Channel Flow, J. of Hyd. Div., ASCE, (1978) 105(HY10)
10. Rozovskii, I.L.: Flow of Water in Bends of Open Channels. Academy of Sciences of the Ukrainian SSR, Kiev., (1957); Israel Program for Scientific Translation, Jerusalem, (1961)
11. Ahmed Shukry: Flow around Bends in an Open Flume, Transactions, ASCE, Vol. 115, (1950) 751-779